

Ab initio lattice dynamics of zinc-blende $\text{Ga}_x\text{In}_{1-x}\text{N}$ alloys

This article has been downloaded from IOPscience. Please scroll down to see the full text article.

2007 J. Phys.: Condens. Matter 19 486209

(<http://iopscience.iop.org/0953-8984/19/48/486209>)

View [the table of contents for this issue](#), or go to the [journal homepage](#) for more

Download details:

IP Address: 129.252.86.83

The article was downloaded on 29/05/2010 at 06:55

Please note that [terms and conditions apply](#).

Ab initio lattice dynamics of zinc-blende $\text{Ga}_x\text{In}_{1-x}\text{N}$ alloys

S Saib^{1,3}, N Bouarissa^{2,4}, P Rodríguez-Hernández¹ and A Muñoz¹

¹ Departamento de Física Fundamental II, Universidad de La Laguna, La Laguna E-38205, Tenerife, Spain

² Department of Physics, Faculty of Science, King Khalid University, Abha, PO Box 9004, Saudi Arabia

E-mail: N.Bouarissa@yahoo.fr

Received 15 July 2007, in final form 21 October 2007

Published 9 November 2007

Online at stacks.iop.org/JPhysCM/19/486209

Abstract

Using *ab initio* calculations in the framework of plane-wave pseudopotential implementation of the density-functional theory within the local density approximation under the virtual crystal approximation, we present a theoretical study of the elastic and dielectric properties and zone-center optical phonons in zinc-blende $\text{Ga}_x\text{In}_{1-x}\text{N}$ alloys over the whole composition range from pure InN to pure GaN. The computed values are generally in reasonably good agreement with the existing experimental data for both parent compounds InN and GaN and provide predictions for $\text{Ga}_x\text{In}_{1-x}\text{N}$ in the composition range 0–1 ($0 < x < 1$). The compositional dependence of the elastic constants, Born effective charge, high-frequency dielectric constant and vibration modes was investigated.

(Some figures in this article are in colour only in the electronic version)

1. Introduction

The group III nitride-based semiconductors and their alloys have attracted considerable attention due to their substantial potential for applications in optoelectronic and high-speed devices operating in the spectral region from the visible to the ultraviolet [1–3]. Gallium and indium nitride (GaN and InN, respectively), like other group III nitrides, have received increasing research interest. In particular, their $\text{Ga}_x\text{In}_{1-x}\text{N}$ alloys offer many possibilities for device engineering, can cover a wide range of wavelengths, and find application in lasers operating in the violet to orange regions of visible light [1, 2, 4]. In addition, GaInN quantum

³ On leave from: Physics Department, Faculty of Science and Engineering, University of M'sila, 28000 M'sila, Algeria.

⁴ Author to whom any correspondence should be addressed.

wells represent a key constituent in the active regions of blue diode lasers and light-emitting diodes [3, 5].

The vast majority of research on III–V nitrides has been focused on a wurtzite crystal phase. The reason is that most III–V nitrides have been grown on sapphire substrates, which generally transfer their hexagonal symmetry to the nitride film. Nevertheless, interest in zinc-blende nitrides has been growing recently [6–14], since it has proved possible to grow nitrides with metastable cubic structure as films using various techniques [15]. The cubic nitrides are also believed to be better suited for doping than the wurtzites. Moreover, it is suggested that the electronic and thermal properties of zinc-blende (cubic) nitrides will be superior to those of the wurtzite materials due to reduced phonon scattering in the high-symmetry crystals [16].

A wide variety of physical properties of solids depend on their lattice dynamical behavior [17]. In addition, properties of interest for device engineering and design are strongly influenced by phonon excitations [18]. Therefore an accurate knowledge of the lattice dynamics is very important for studying phenomena related to electron–phonon interactions, such as the resistivity of metals, superconductivity, and the temperature dependence of optical spectra to name a few (for a review see [17]). Although a number of experimental and theoretical studies of the electronic structure and some related properties of $\text{Ga}_x\text{In}_{1-x}\text{N}$ ternary alloys have been reported [19–24], to the best of our knowledge there are no data for lattice dynamical properties of $\text{Ga}_x\text{In}_{1-x}\text{N}$ in the zinc-blende structure.

In the present paper we present an *ab initio* study of the elastic, dielectric and vibrational properties of the zinc-blende $\text{Ga}_x\text{In}_{1-x}\text{N}$ alloys over the whole range of Ga concentration x , using state-of-the art density-functional theory (DFT) within the local density approximation (LDA). The LDA approximation has turned out to be much more successful than originally expected [25], in spite of its extreme simplicity. For weakly correlated materials, such as semiconductors and simple metals, the LDA accurately describes structural and vibrational properties: the correct structure is usually found to have the lowest energy, while bond lengths, bulk moduli, and phonon frequencies are accurate to within a few per cent [17]. The dynamical properties of the alloy are treated within the virtual crystal approximation (VCA). We report results regarding elastic constants, Born effective charge, high-frequency dielectric constant, and the zone-center phonon frequencies and their composition dependence in the zinc-blende $\text{Ga}_x\text{In}_{1-x}\text{N}$ ternary alloys.

2. Computational method

The calculations were performed using a first-principles pseudopotential method based on the DFT [26] within the LDA with the Ceperley–Alder form [27] of the exchange–correlation energy density of a homogeneous gas as parameterized by Perdew and Wang [28]. The pseudopotentials were generated by adopting the scheme described by Troullier and Martins [29]. Both of the 3d electrons of Ga and the 4d electrons of In are treated as valence electrons. Well-converged results were obtained with the consideration of the kinetic energy cutoff of 160 Ryd, and a mesh of $6 \times 6 \times 6$. All the reciprocal-space integrations were performed using the Monkhorst–Pack scheme [30]. To determine the equilibrium geometry of the zinc-blende phase, we optimize the volume of the unit cell (V). The variation of the total energy per atom as a function of volume is then fitted to Murnaghan’s equation of state so as to determine the equilibrium structural parameters. The obtained volumes for InN and GaN are 30.51 and 22.78 Å³, respectively. The estimated values from the experimental data reported in [31] are 30.88 and 22.63–23.09 Å³ for InN and GaN, respectively. These values agree with ours to within 2%.

Table 1. The calculated elastic constants for zinc-blende InN, Ga_{0.50}In_{0.50}N and GaN.

Material	Elastic constants (GPa)		
	C_{11}	C_{12}	C_{44}
InN	181 ^a ; 216.32 ^b ; 187 ^c ; 184 ^d ; 183 ^e ;	124 ^a ; 94.12 ^b ; 125 ^c ; 116 ^d ; 124 ^e ;	130 ^a ; 98.14 ^b ; 86 ^c ; 177 ^d ; 86 ^e ;
Ga _{0.50} In _{0.50} N	210 ^a ; 264.14 ^b	132 ^a ; 115.28 ^b	147 ^a ; 119.66 ^b
GaN	296 ^a ; 320.03 ^b ; 293 ^c ; 296 ^d ; 287 ^e ;	159 ^a ; 140.31 ^b ; 159 ^c ; 154 ^d ; 158 ^e ;	200 ^a ; 144.64 ^b ; 155 ^c ; 206 ^d ; 159 ^e ;

^a Present work.^b Theory: reference [35].^c Theory: reference [36].^d Theory: references [37, 38].^e Theory (LDA results): reference [39].

The phonon frequencies and atomic displacements were subsequently obtained using the linear response method, which avoids the use of supercells and allows the calculation of the dynamical matrix at arbitrary q vectors. The eigen-frequencies and eigen-vectors of the lattice vibrations were calculated within the framework of the self-consistent density-functional perturbation theory (DFPT) [32–34]. State-of-the-art DFPT [32] provides an accurate and efficient way to compute the vibrational properties of crystalline materials. For an alloy, this technique needs large supercells so as to simulate the effects of disorder. In the present study, the VCA has been used for the alloy of interest in the zinc-blende structure. The interatomic force constants were obtained with a Fourier transform of the dynamical matrix on a discrete mesh of spacing. The interatomic force constants thus obtained can be used to compute the dynamical matrices at an arbitrary q point. A kinetic energy cutoff and a special point set ensure the convergence of the phonon frequencies to within 2 cm^{-1} with the same grid and kinetic energy cutoff mentioned above.

3. Results and discussion

3.1. Elastic properties

The effect of strain on electronic properties requires knowledge of the material's mechanical properties, and specifically the elastic constants which describe the response to an applied macroscopic stress. In table 1, we present our results for the elastic constants of zinc-blende InN, GaN, and Ga_{0.50}In_{0.50}N. Also shown for comparison are other published data in the literature. Note that while the present results differ from those of the empirical pseudopotential calculation reported in [35], they agree generally reasonably well with the theoretical analysis of Wright [36] and the results of *ab initio* calculations within the LDA reported by Lepkowski *et al* [39]. However, the agreement for C_{44} is not as good as for C_{11} and C_{12} . The reason for this could be attributed to the fact that the present calculations are performed using DFPT whereas those of Wright were based on the lattice deformation method. Similar sets were almost calculated by Kim *et al* [37, 38] using the full-potential linear muffin-tin orbital method.

The compositional dependence of the elastic constants, namely C_{11} , C_{12} and C_{44} , is plotted in figure 1. Note that all elastic constants (C s) of interest increase with increasing Ga content. However, the rate of increase seems to be larger for C_{11} . A similar trend has been reported by Bouarissa and Kassali [35] using the empirical pseudopotential method under the VCA. Assuming that the C versus x curves are quadratic, one defines the C s by the relation

$$C(x) = (1 - x)C(0) + xC(1) - bx(1 - x), \quad (1)$$

where b is the elastic constant bowing parameter. The latter can be determined by making a polynomial fit of order two of the elastic constant data using a least-squares procedure. The

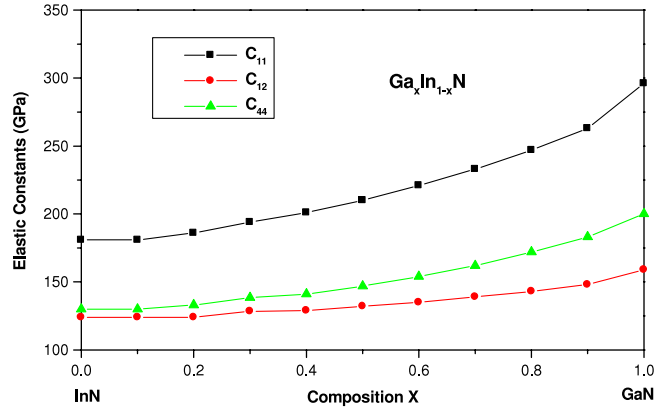


Figure 1. Elastic constants of zinc-blende $\text{Ga}_x\text{In}_{1-x}\text{N}$ versus composition x .

Table 2. Calculated bowing parameters of elastic constants (C_{11} , C_{12} and C_{44}), macroscopic dielectric constant ($\epsilon(\infty)$), Born effective charge (z^B) and zone-center phonon frequencies (ω_{TO} and ω_{LO}) for zinc-blende $\text{Ga}_x\text{In}_{1-x}\text{N}$.

Physical quantity	Bowing parameter
C_{11} (GPa)	107.93
C_{12} (GPa)	36.01
C_{44} (GPa)	69.35
z^B	-0.28
$\epsilon(\infty)$	-3.72
ω_{TO} (cm^{-1})	99.28
ω_{LO} (cm^{-1})	156.41

obtained bowing parameters of the elastic constants are given in table 2. The C_{11} bowing parameter is larger than those of C_{12} and C_{44} , thus confirming that the rate of increase of C_{11} discussed previously is larger than that of C_{12} and C_{44} . On the other hand, one can note that the values of these bowing parameters are much larger than those generally reported for III-V ternary semiconductor alloys [40–42]. This trend has also been reported for the elastic constants in the ternary alloy $\text{Sc}_x\text{Ga}_{1-x}\text{N}$ [43] with the zinc-blende structure.

3.2. Dielectric properties

Contrary to the non-polar IV-IV element crystals, atomic displacements in polar materials create dipoles. This gives rise to long-range force constants in real space and to the non-analytic behavior of the dynamical matrix at Γ [44]. To deal with the macroscopic electric field associated with the longitudinal optical modes and the related non-analytic behavior of the dynamical matrix at Γ , we have studied the dielectric tensor $\epsilon(\infty)$ and the Born effective-charge $Z^B(\kappa)$ tensor for the material of interest at various Ga concentrations ranging from 0 to 1. In the present study the zinc-blende phase has been considered. Thus, the tensor of $Z^B(\kappa)$ is isotropic. On the other hand, due to the neutrality of charges, the cation and anion charges only differ by their sign. Our results regarding $\epsilon(\infty)$ and Z^B for InN and GaN are listed in table 3. For comparison, available data from the literature are also included. In terms of previous theoretical calculation, when comparing our results regarding $\epsilon(\infty)$ with those of Christensen and Gorczyca [45], which are the only available data to our knowledge for InN,

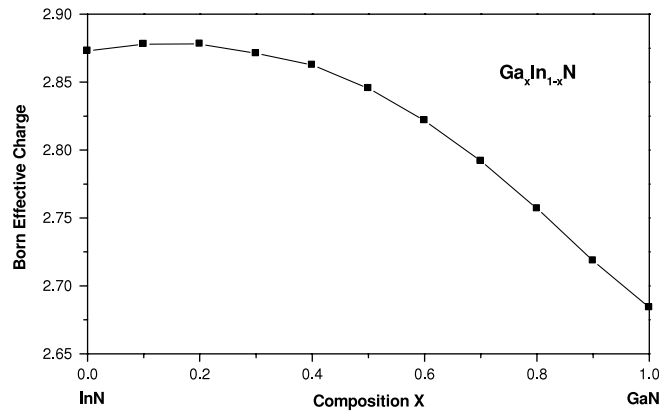


Figure 2. Born effective charge of zinc-blende $\text{Ga}_x\text{In}_{1-x}\text{N}$ versus composition x .

Table 3. Macroscopic dielectric constant $\varepsilon(\infty)$ and Born effective charge Z^B for zinc-blende InN and GaN.

Material	$\varepsilon(\infty)$	Z^B
InN	8.09 ^a ; 6.15 ^b	2.87 ^a
GaN	6.09 ^a ; 4.78 ^b ; 5.41 ^c ; 5.29 ^d ; 5.3 ^e ; 5.2 ^f ; 5.7 ^g	2.68 ^a 2.65 ^c

^a Present work.

^b Theory: reference [45].

^c Theory: reference [46].

^d Expt.: reference [47].

^e Expt.: reference [48].

^f Expt.: reference [49].

^g Expt.: reference [50].

we note that our values are larger than those reported in [45]. This is quite surprising since in our calculations local-field effects are taken into account, whereas the authors of [45] did not include in their calculations the local-field effects which in principle reduce the dielectric constant [46]. For zinc-blende GaN, the agreement between our results regarding $\varepsilon(\infty)$ and the theoretical ones reported by Karch *et al* [46] is within 13%. The experimental data for $\varepsilon(\infty)$ of zinc-blende GaN lie within a range of 5.2–5.7 [47–50], showing a good agreement with our results to within 6%–18%. As regards Z^B , the only available data for comparison are those reported by Karch *et al* [46] for zinc-blende GaN. Excellent agreement can be noticed between our result and that of [46].

Recently Bungaro *et al* [18] reported that in the zinc-blende structure, the group III nitrides follow the same trend as the static ionicities, as measured by the charge asymmetry coefficients, suggesting that InN has larger dynamical and static ionicities than GaN. This trend is consistent with our results.

The variation of Z^B in zinc-blende $\text{Ga}_x\text{In}_{1-x}\text{N}$ as a function of Ga content is plotted in figure 2, whereas that of $\varepsilon(\infty)$ is depicted in figure 3. Note that as the Ga concentration increases from 0 to 1 (on going from InN to GaN), Z^B increases slightly up to $x = 0.2$ then decreases monotonically. The same conclusion can be drawn for the qualitative behavior of $\varepsilon(\infty)$. Using a similar form of equation (1), Z^B and $\varepsilon(\infty)$ as a function of x can be represented by quadratic relations; the corresponding bowing parameters of Z^B and $\varepsilon(\infty)$ are given in table 2.

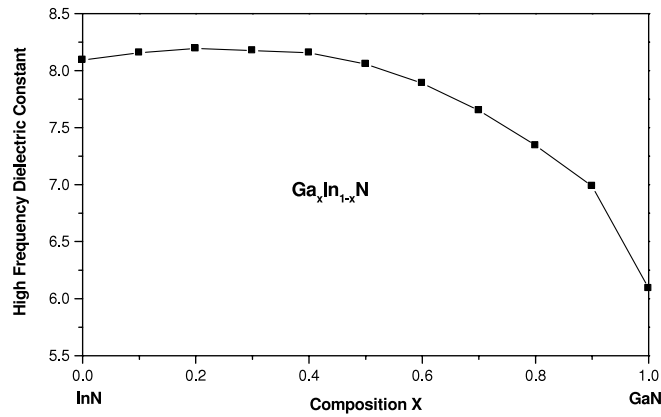


Figure 3. High-frequency dielectric constant of zinc-blende $\text{Ga}_x\text{In}_{1-x}\text{N}$ versus composition x .

Table 4. Zone-center phonon frequencies in units of cm^{-1} for zinc-blende InN and GaN.

Material	ω_{TO}	ω_{LO}
InN	465 ^a ; 478 ^b	566 ^a ; 694 ^b
GaN	545 ^a ; 580 ^b ; 560 ^c ; 558 ^d ; 551 ^e ; 555 ^f ; 552 ^g	718 ^a ; 750 ^c ; 743 ^g ; 741 ^h ; 740 ^{i,k} ; 739 ^j

^a Present work.

^b Theory: reference [38].

^c Theory: reference [46].

^d Theory: reference [51].

^e Theory: reference [52].

^f Expt.: references [47, 54, 55].

^g Expt.: reference [53].

^h Expt.: reference [47].

ⁱ Expt.: reference [54].

^j Expt.: reference [48].

^k Expt.: reference [55].

3.3. Vibrational properties

Accurate description of vibrational properties is extremely important in the study of transport and optical properties in polar semiconductors and results in a better understanding of structural parameters responsible for the efficiency of optical devices.

In the cubic cases one has to deal only with the most important frequencies, ω_{LO} and ω_{TO} at the Γ point. Our computed results regarding the zone-center phonon frequencies for zinc-blende InN and GaN are shown in table 4. For comparison experimental and theoretical data available are also presented. For zinc-blende InN, the only available data in the literature are those calculated by Kim *et al* [38] using first-principles full-potential linear muffin-tin orbital method. The agreement between our results and those of [38] as regards ω_{LO} and ω_{TO} is better than 3% and 19%, respectively. For zinc-blende GaN, the agreement between our result and the previously calculated data as regards ω_{TO} is reasonably good, whereas for ω_{LO} the agreement between our result and that reported by Karch *et al* [46] using first-principles calculations within the LDA is better than 5%. In terms of experimental results, the computed phonon frequencies of both InN and GaN at the Γ point agree very well with the average of the measured Raman frequencies from [47, 48, 53–55].

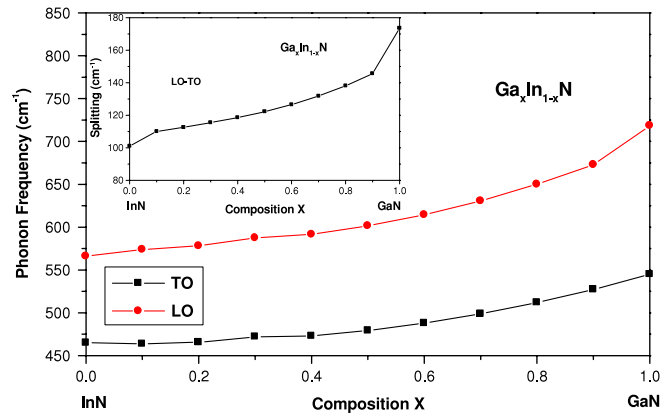


Figure 4. Zone-center optical frequencies for zinc-blende $\text{Ga}_x\text{In}_{1-x}\text{N}$ versus composition x . Inset: difference frequencies of LO and TO phonons for zinc-blende $\text{Ga}_x\text{In}_{1-x}\text{N}$ versus composition x .

In figure 4, the transverse optical (TO) and the longitudinal optical (LO) frequencies are plotted against Ga content for zinc-blende $\text{Ga}_x\text{In}_{1-x}\text{N}$. Note that with increasing Ga concentration over the whole compositional range from pure InN to pure GaN, the LO phonon frequency increases monotonically whereas the TO phonon frequency decreases slightly up to $x = 0.1$ then increases monotonically up to $x = 1$. Similar behavior has been reported by Boucenna and Bouarissa [56] for LO and TO phonon frequencies in $\text{InAs}_x\text{Sb}_{1-x}$ ternary alloys using the empirical pseudopotential method under the VCA combined with the Harrison bond orbital model. Using the same form of equation (1), one obtains the bowing parameters of TO and LO phonon frequencies that are shown in table 2.

It is worth noting from figure 4 that the variation of the TO and LO frequency versus x reflects the widening of the LO–TO splittings as one proceeds from InN to GaN as shown in the inset in figure 4. The LO–TO splitting characterizes the long-range electrostatic forces on the atoms of the vibrating lattice. The non-vanishing LO–TO splitting at the zone-center is related to its partial ionic bonding. In fact, the ionicity reveals itself in the splitting of the LO and TO modes. However, the increasing LO–TO splitting in the present case for $\text{Ga}_x\text{In}_{1-x}\text{N}$ on going from pure InN to pure GaN is not due to an increase in ionicity since according to the Phillips ionicity scale [57], the ionicity factor of InN is 0.578 and that of GaN is 0.50 (i.e. according to [57] InN is more ionic than GaN). The same conclusion has been drawn by Wagner and Bechstedt [58] for the behavior of LO–TO splitting with hydrostatic pressure in group III nitrides, which in turn is in contrast to the behavior of most of other III–V semiconductors under pressure [59].

4. Conclusion

In summary, we have reported dielectric and lattice dynamical properties of zinc-blende $\text{Ga}_x\text{In}_{1-x}\text{N}$ mixed crystals over the whole composition range from pure InN to pure GaN, by means of first-principles pseudopotential plane-wave method based on the DFT within the LDA. We find generally good agreement with previous calculations and the available experimental data for both compounds InN and GaN. The present calculations for $\text{Ga}_x\text{In}_{1-x}\text{N}$ alloys in the composition range 0–1 ($0 < x < 1$) provide predictions of the studied properties. The elastic constants are found to increase non-linearly with increasing Ga concentration, showing a large bowing parameter. The Born effective charge showed the

same qualitative behavior with respect to x as that of the high-frequency dielectric constant. The compositional dependence of the zone-center optical phonons showed that the LO mode increases monotonically from InN to GaN, whereas the TO mode decreases slightly up to $x = 0.1$ then increases up to $x = 1$, suggesting thus that LO–TO splitting becomes larger as one goes from InN to GaN. This behavior cannot be explained by the increase of the ionicity, which according to the Phillips ionicity scale decreases as one proceeds from InN to GaN.

While the present calculations still leave a doubt about the validity because of the VCA, it might be worthwhile checking with further work. Therefore, further experimental measurements and supercell calculations that simulate the effects of disorder are needed in order to obtain more accurate and reliable results for the (GaIn)N system.

Acknowledgment

One of us (SS) would like to express her gratitude to the staff of the Departamento de Física Fundamental II, Universidad de La Laguna, Tenerife, Spain, for their kind hospitality extended during her stay at Tenerife and their help whenever possible.

References

- [1] Orton J W and Foxon C T 1998 *Rep. Prog. Phys.* **61** 1
- [2] Jain S C, Willander M, Narayan J and van Overstraeten R 2000 *J. Appl. Phys.* **87** 965
- [3] Vurgaftman I and Meyer J R 2003 *J. Appl. Phys.* **94** 3675
- [4] O'Donnell K P, Martin R W and Middleton P G 1999 *Phys. Rev. Lett.* **82** 237
- [5] Nakamura S and Fasol G (ed) 1997 *The Blue Laser Diode* (Berlin: Springer)
- [6] Lei T, Fanciulli M, Molnar R J, Moustakas T D, Graham R J and Scanlon J 1991 *Appl. Phys. Lett.* **59** 944
- [7] Strite S, Ruan J, Li Z, Salvador A, Chen H, Smith D J, Choyke W J and Morkoc H 1991 *J. Vac. Sci. Technol.* **9** 1924
- [8] Strite S and Morkoc H 1992 *J. Vac. Sci. Technol. B* **10** 1237
- [9] Ploog K H, Brandt D, Yang H, Menniger J and Klann R 1997 *Solid-State Electron.* **41** 235
- [10] Tsuchiya H, Takeuchi A, Matsuo A and Hasegawa F 1997 *Solid-State Electron.* **41** 333
- [11] Bouarissa N 2002 *Phys. Status Solidi b* **231** 391
- [12] Bouarissa N 2002 *Eur. Phys. J. B* **26** 153
- [13] Saib S and Bouarissa N 2005 *Eur. Phys. J. B* **47** 379
- [14] Saib S and Bouarissa N 2007 *Physica B* **387** 377
- [15] Hong C H, Pavlidis D, Brown S W and Rand S C 1995 *J. Appl. Phys.* **77** 1705
- [16] Schwoerer-Böhning M, Macrander A T, Pabst M and Pavone P 1999 *Phys. Status Solidi b* **215** 177
- [17] Baroni S, de Gironcoli S, Dal Corso A and Giannozzi P 2001 *Rev. Mod. Phys.* **73** 515
- [18] Bungaro C, Rapcewicz K and Bernholc J 2000 *Phys. Rev. B* **61** 6720
- [19] Tsujimura A, Hasegawa Y, Ishibashi A, Kamigama S, Kidoguchi I, Miyanaga R, Suzuki M, Kume M, Harafuji K and Ban Y 1999 *Electron. Lett.* **35** 998
- [20] Kassali K and Bouarissa N 2000 *Solid-State Electron.* **44** 501
- [21] Bouarissa N 2000 *Phil. Mag. B* **80** 1743
- [22] Wetzel C, Kamiyama S, Amano H and Akasaki I 2002 *Japan. J. Appl. Phys.* **1** **41** 11
- [23] Bhouri A, Mejri H, Ben Zid F, Belmabrouk H, Said M, Bouarissa N and Lazzari J-L 2004 *J. Phys.: Condens. Matter* **16** 511
- [24] Neubert B, Bruckner P, Habel F, Scholz F, Riemann T, Christen J, Beer M and Zweek J 2005 *Appl. Phys. Lett.* **87** 182111
- [25] Jones R O and Gunnarson O 1989 *Rev. Mod. Phys.* **61** 689
- [26] Gonze X, Beuken J-M, Caracas R, Detraux F, Fuchs M, Rignanese G-M, Sindic L, Verstraete M, Zerah G, Jollet F, Torrent M, Roy A, Mikami M, Ghosez P, Raty J-Y and Allan D C 2002 *Comput. Mater. Sci.* **25** 478
- [27] Ceperley D M and Alder B J 1980 *Phys. Rev. Lett.* **45** 566
- [28] Perdew J P and Wang Y 1992 *Phys. Rev. B* **45** 13244
- [29] Troullier N and Martins J L 1991 *Phys. Rev. B* **43** 1993
- [30] Monkhorst H J and Pack J D 1976 *Phys. Rev. B* **13** 5188

- [31] Serrano J, Rubio A, Hernandez E, Muñoz A and Mujica A 2000 *Phys. Rev. B* **62** 16612 and references therein
- [32] Baroni S, Giannozzi P and Testa A 1987 *Phys. Rev. Lett.* **58** 1861
- [33] Giannozzi P, de Gironcoli S, Pavone P and Baroni S 1991 *Phys. Rev. B* **43** 7231
- [34] Karch K, Bechstedt F, Pavone P and Strauch D 1996 *Phys. Rev. B* **53** 13400
- [35] Bouarissa N and Kassali K 2001 *Phys. Status Solidi b* **228** 663
Bouarissa N and Kassali K 2002 *Phys. Status Solidi b* **231** 294 (erratum)
- [36] Wright A F 1997 *J. Appl. Phys.* **82** 2833
- [37] Kim K, Lambrecht W R L and Segall B 1994 *Phys. Rev. B* **50** 1502
- [38] Kim K, Lambrecht W R L and Segall B 1996 *Phys. Rev. B* **53** 16310
- [39] Lepkowski S P, Majewski J A and Jurczak G 2005 *Phys. Rev. B* **72** 245201
- [40] Adachi S 1985 *J. Appl. Phys.* **58** R1
- [41] Bouarissa N 2003 *Mater. Sci. Eng. B* **100** 280
- [42] Bouarissa N 2006 *Mater. Chem. Phys.* **100** 41
- [43] Oussaifi Y, Ben Fredj A, Debbichi M, Bouarissa N and Said M 2007 *Semicond. Sci. Technol.* **22** 641
- [44] Karch K and Bechstedt F 1997 *Phys. Rev. B* **56** 7404
- [45] Christensen N E and Gorczyca I 1994 *Phys. Rev. B* **50** 4397
- [46] Karch K, Wagner J-M and Bechstedt F 1998 *Phys. Rev. B* **57** 7043
- [47] Azuhata T, Sota T, Suzuki K and Nakamura S 1995 *J. Phys.: Condens. Matter* **7** L129
- [48] Giehler M, Ramsteiner M, Brandt O, Yang H and Ploog K H 1995 *Appl. Phys. Lett.* **67** 733
- [49] Ejder E 1971 *Phys. Status Solidi a* **5** 445
- [50] Perlin P, Jauberthie-Carillon C, Itie J P, San Miguel A, Grzegory I and Polian A 1992 *Phys. Rev. B* **45** 83
- [51] Miwa K and Fukumoto A 1993 *Phys. Rev. B* **48** 7897
- [52] Gorczyca I, Christensen N E, Blanca E L P Y and Rodriguez C O 1995 *Phys. Rev. B* **51** 11936
- [53] Tabata A, Enderlein R, Leite J R, da Silva S W, Galzerani J C, Schikora D, Kloidt M and Lischka K 1996 *J. Appl. Phys.* **79** 4137
- [54] Siegle H, Eckey L, Hoffmann A, Thomson C, Meyer B K, Schikora D, Hankeln M and Lischka K 1995 *Solid State Commun.* **96** 943
- [55] Cros A, Dimitov R, Aagerer H, Ambacher O, Stutzmann M, Christiansen S, Albrecht M and Strunk H P 1997 *J. Cryst. Growth* **181** 197
- [56] Boucenna M and Bouarissa N 2007 *Mater. Sci. Eng. B* **138** 228
- [57] Phillips J C 1973 *Bonds and Bands in Semiconductors* (New York: Academic)
- [58] Wagner J-M and Bechstedt F 2000 *Phys. Rev. B* **62** 4526
- [59] Bouarissa N, Bougouffa S and Kamli A 2005 *Semicond. Sci. Technol.* **20** 265